A Conic Sector-Based Methodology for Nonlinear Control Design

Francis J. Doyle III and Manfred Morari*

Chemical Engineering 210-41
California Institute of Technology
Pasadena CA 91125

Abstract

A design method is presented for the analysis and synthesis of robust nonlinear controllers for chemical engineering systems. The method rigorously treats the effect of unmeasured disturbances and unmodeled dynamics on the stability and performance properties of a nonlinear system. The results utilize new extensions of structured singular value theory for analysis and recent synthesis results for approximate linearization.

1 Introduction

There has been considerable interest in the application of differential geometry to the control of nonlinear process systems over the past five years. The inherently nonlinear nature of chemical process dynamics and the pathological behavior which can evolve from these systems has motivated the application of these techniques to process control. Two of the more popular approaches, state linearization and input-output linearization, have received considerable attention. With a few notable exceptions [1], the issues of unmeasured disturbances and unmodeled dynamics in these frameworks have not been properly emphasized. In this paper we propose a general methodology to address these issues.

The analysis tools employed in this research are extensions of the structured singular value (SSV) to nonlinear systems [3],[10]. Utilizing the conic sector approximation of a nonlinear operator, it is possible to represent a nonlinear system as a nominal LTI plant perturbed by a bounded nonlinear operator. The SSV results for nonlinear perturbations are only sufficient and thus conservative. Therefore, the primary objective in this design scheme is the minimization of the size of the nonlinear perturbations. This is accomplished by two means. First, the nonlinear nature of the plant is minimized by means of approximate linearization via state transformation and feedback [9]. Second, a tight characterization of the resultant nonlinearity is achieved with an optimization program. Thus, we arrive at a nearly "linear" plant description which can then be handled with standard robust linear control theory.

The usual Euclidean norm or 2-norm will be used to calculate the norm of vectors in $\mathcal{C}^n$ or $\mathcal{R}^n$. For vector signals $e(t)$ this norm is defined to be: $\|e(t)\|^2 = \int_{-\infty}^{\infty} e^T(t)e(t)dt$. The operator norm induced by the 2-norm is:

$$\sup_{\substack{v\neq 0 \\ v\in\mathcal{L}_2}} \frac{\|Gv\|}{\|v\|} = \sup_{\omega} \bar{\sigma}(G(j\omega)) \triangleq \|G\|_\infty \tag{1}$$

where $\mathcal{L}_2$ is the space of functions with bounded 2-norm. This is also the operator norm induced by the power norm defined to be: $\|e(t)\|_p^2 = \lim_{\tau\to\infty} \int_{-\tau}^{\tau} \frac{1}{2\tau} e^T(t)e(t)dt$. The Frobenius norm for matrices in $\mathcal{C}^{n\times n}$ is given by $\|A\|_F = \left[\sum_i \sum_j |a_{ij}|^2\right]^{\frac{1}{2}}$. The superscript notation, $f^{(\rho)}(x)$, will be used to represent a polynomial function of order ρ in the argument.

2 Feedback Linearization

The general problem focuses on control-linear systems of the form:

$$\dot{x} = f(x) + g(x)u + d(x,t) \tag{2}$$

where $x \in \Re^n$, $u \in \Re^m$ and $d \in \Re^n$. Here, $d(x,t)$ may represent external disturbances as well as unmodeled dynamics : the key point is that it is unmeasured. The general state and input transformations

$$z = T(x) \tag{3}$$
$$u = \alpha(x) + (I + \beta(x))v \tag{4}$$

transform (2) to one of several forms depending upon the selected technique.

We consider here a comparison of the Global State Linearization [5] (GSL) technique and the Approximate Linearization (AL) developed by Krener and co-workers [7], [9]. Using the following features as measures, the AL represents a ***significantly*** superior linearization approach:

- Transformed Coordinate System
- Disturbance Effects
- Involutivity Restrictions
- Optimization of Possible Transformations

These issues will now be discussed in more detail.

2.1 Transformed Coordinate System

GSL transforms systems of the form (2) into the following dynamical system:

$$\dot{z} = \begin{pmatrix} 0 & 1 \\ 0 & 0 \end{pmatrix} z + \begin{pmatrix} 0 \\ 1 \end{pmatrix} v + \left[\frac{\partial T}{\partial x} d(x,t)\right]_{x=T^{-1}(z)} \tag{5}$$

Although the resultant nominal state dynamics are linear, they are in Brunovsky canonical form in which many of the states have lost their physical significance. For process systems in which the states are typically temperatures and concentrations, the transformed variables may represent unmeasurable quantities or highly nonlinear functions of the measurable variables. Another problem with the so called "global" techniques is the fact that the state transformation $T(x)$ is only a local diffeomorphism and therefore these techniques can only be applied over finite regions of the phase space.

AL also handles systems of the form in (2), but for convenience we will represent the nominal system as a series expansion of the terms in equation (2):

$$\dot{x} = Fx + f^{(2)}(x) + \cdots + f^{(\rho)}(x) + \left(G + g^{(1)}(x) + \cdots + g^{(\rho-1)}(x)\right)u + O^{(\rho+1)}(x,u) \tag{6}$$

The following structure is imposed upon the state transformation:

$$z = x - \phi^{(\rho)}(x) \tag{7}$$

The resultant dynamical system is linear in the state dynamics up through order ρ terms:

$$\dot{z} = Fz + Gv + \left[\frac{\partial T}{\partial x} d(x,t)\right]_{x=T^{-1}(z)} + O^{\rho+1}(z,v) \tag{8}$$

This particular choice of state transformation (7) and input (4) transformation leads to first order terms F and G which are identical to the respective terms in the first order approximation of the original dynamical system. Technically, we say that the new variables z have ρth-order contact with the original variables x. This is

*Author to whom correspondence should be addressed: mm@imc.caltech.edu, (818)356-4186

contrasted with the GSL in which the transformed coordinates have only zero order contact with the original variables (higher derivatives do not match). The implications for control design are obvious. We can calculate optimal linear controllers for the first order approximation of our original system and apply them directly to the AL system. For the GSL approach, one must first translate the desired first order dynamics in x to the new coordinate system before the corresponding linear control law can be calculated.

2.2 Disturbance Effects

Another weakness of the GSL technique is revealed in the incorporation of disturbances and unmodeled dynamics into the transformed coordinates. It can be seen in equation (5) that even simple linear disturbances are transformed into potentially pathological operators in the linearized coordinate system. Simple perturbations in d may dramatically effect the already critically stable nominal system (open loop). This is contrasted with the AL approach in which the transformation Jacobian matrix has zero-order terms equal to identity. The higher order terms are simple polynomials in x. In effect, this minimizes the "nonlinear" nature of the disturbances.

2.3 Involutivity Restrictions

A resriction on the nonlinear systems which admit GSL solutions is an involutivity condition, the computation of which becomes quite difficult for large order systems. Typical chemical engineering processes, particularly complex reaction systems, violate this constraint [8]. In contrast, the AL approach requires only that the system be "approximately involutive" or order-ρ involutive [9]. This is a milder constraint in the sense that it allows an order ρ remainder term whereas GSL requires zero remainder.

2.4 Optimization of Possible Transformation

One of the real strengths of the AL approach lies in its flexibility to "optimize" the resultant solution. Consider the mapping from the transformations (ϕ, α, β) to the functions (f, g). For AL, one can represent this mapping in terms of the polynomial coefficients of the various polynomial functions. (A straightforward interpretation is not possible for the GSL.) If this mapping has a non-trivial kernel, then a parametrized family of solutions results. The parameters are selected to minimize the "size" of α, β and ϕ. If the magnitude of ϕ is minimized, then the mapping from x to z becomes closer to identity. Similarly, minimizing α and β yields a mapping from u to v that is close to identity. Thus the linearization is accomplished with *minimal* nonlinear "distortion" of the original system.

Similarly, if the map is deficient in rank, then a linearization solution is not possible (i.e. the system is not ρ-order involutive). In this case, one can search over the space of solutions $(\tilde{f}, \tilde{g})$ which *are* linearizable. An optimization is done to minimize the distance between (f, g) and $(\tilde{f}, \tilde{g})$. The reader is referred to [7] for the optimization algorithm and a discussion of the relevant metrics used to define the various sizes and distances.

In effect, the constraint in section 2.3 is removed. This will be demonstrated with a non-involutive example in the next section. This systematic procedure for finding the "closest" linearizable system reveals the flexibility of the AL approach.

2.5 Summary

It has been shown in equations (5) and (8) how the so-called linearization techniques actually result in nonlinear systems when the effects of disturbances and unmodeled dynamics are accounted for. This is represented in Figure 1 where the shaded blocks are nonlinear operators. At the center of this structure are the input transformation, nonlinear plant, and state transformation. It is clear to see the effect of unmodeled dynamics and disturbances on the stability of the open loop transformed system. Δ_1 represents the difference between the true nonlinear dynamics and the assumed model. For instance, the Quadratic Approximate Linearization scheme (QAL), $\rho = 2$, has a Δ_1 term to represent order 3 and higher effects. Δ_2 represents the nonlinear effect of the disturbance acting through the Jacobian of the transformation. Finally, Δ_3 represents the nonlinearity associated with the actual coordinate transformation itself and its effect upon the set-point signal.

The preceding four sections have clearly enumerated the incentives for using Approximate Linearization. This overall practicality

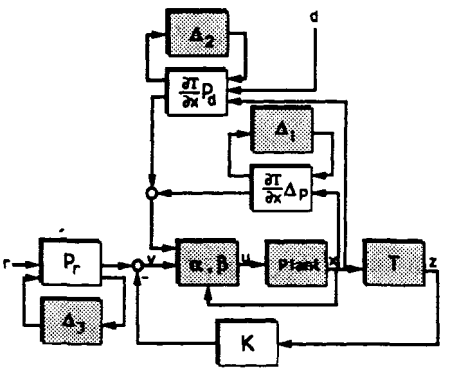

Figure 1: General Linearization Structure

motivates its use in the present design. In addition, there are extensions of this technique to systems in which the outputs are nonlinear functions of the states. Although they are not explored here, they represent an attractive framework for pursuing input-output linearization.

2.6 Application to a Non-Involutive System

Consider a continuous stirred tank reactor (CSTR) in which the following isothermal, liquid-phase chemical reactions take place :

$$A \overset{1,2}{\rightleftharpoons} B \overset{3,4}{\rightleftharpoons} C \tag{9}$$

The following rate expressions hold: $r_1 = k_1 C_A, r_2 = k_2 C_B^2, r_3 = k_3 C_B^2$ and $r_4 = k_4 C_C$. Manipulation of the concentration of C (desired output) will be accomplished by the flow rate of a feedback stream consisting of primarily component B which has been separated from the aqueous solution by a drying process. The following choice of physical parameters ($\mathcal{D}a_1 = 3.0, \mathcal{D}a_2 = 0.5, \mathcal{D}a_3 = 1.0, \mathcal{D}a_4 = 2.0, \lambda_a = 0.1, \lambda_b = 0.75, \lambda_c = 0.15$) and operating point ($u_{f0} = .5, x_{a0} = 0.33, x_{b0} = 0.79, x_{c0} = 0.21$) leads to the normalized dimensionless mass balances:

$$\dot{\tilde{x}} = \begin{pmatrix} -3.95 & .790 & 0.0 \\ 3.0 & 2.994 & 2.0 \\ 0.0 & 1.580 & -2.925 \end{pmatrix} \tilde{x} + \begin{pmatrix} .033 \\ .592 \\ .032 \end{pmatrix} \tilde{u}$$
$$+ \begin{pmatrix} .5\tilde{x}_b^2 \\ -1.5\tilde{x}_b^2 \\ 1.0\tilde{x}_b^2 \end{pmatrix} + \begin{pmatrix} 0.1 & 0.0 & 0.0 \\ 0.0 & 0.75 & 0.0 \\ 0.0 & 0.0 & 0.15 \end{pmatrix} \begin{pmatrix} \tilde{x}_a \\ \tilde{x}_b \\ \tilde{x}_c \end{pmatrix} \tilde{u} \tag{10}$$

Note that this system is second order and is in control-linear form. However, it is straightforward to show that this system is not involutive. Using the MATLAB software for QAL (see Acknowledgements) one sees that the following plant is in fact involutive:

$$\dot{\tilde{x}} = \begin{pmatrix} -3.95 & .790 & 0.0 \\ 3.0 & 2.994 & 2.0 \\ 0.0 & 1.580 & -2.925 \end{pmatrix} \tilde{x} + \begin{pmatrix} .033 \\ .592 \\ .032 \end{pmatrix} \tilde{u}$$
$$+ \begin{pmatrix} -.00058\tilde{x}_a\tilde{x}_b & .490\tilde{x}_b^2 & -.00056\tilde{x}_b\tilde{x}_c \\ & -1.5\tilde{x}_b^2 & \\ .00027\tilde{x}_a\tilde{x}_b & 1.005\tilde{x}_b^2 & .00026\tilde{x}_b\tilde{x}_c \end{pmatrix} \tag{11}$$
$$+ \begin{pmatrix} 0.112 & -0.012 & 0.027 \\ -.00039 & 0.750 & -.00086 \\ -.0052 & 0.011 & 0.138 \end{pmatrix} \begin{pmatrix} \tilde{x}_a \\ \tilde{x}_b \\ \tilde{x}_c \end{pmatrix} \tilde{u}$$

The remarkable closeness of the two systems is attributable to a remainder term which satisfies the approximate involutivity condition for system (11). Simulation results confirm that when the QAL for (11) is applied to (10), the resultant closed loop exhibits less nonlinear behavior than the original nonlinear plant with simple linear control [2].

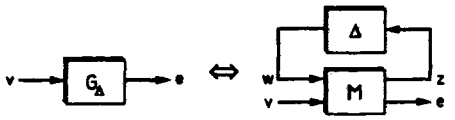

Figure 2: General Framework for SSV Analysis

3 Structured Singular Value Concepts

3.1 General Framework

We consider the system shown in Figure 2 where M(s) is a linear time invariant operator and Δ is a nonlinear operator with the following block structure:

$$\mathbf{\Delta} \triangleq \{\text{diag}[\delta_1 I_{r_1}, \ldots, \delta_m I_{r_m}, \Delta_1, \ldots, \Delta_n]\} \tag{12}$$

This structure can be arrived at from any interconnection of linear blocks and nonlinear perturbations, Δ. In the diagram, the input v represents set points, disturbances and noise, the output e represents error signals. In this framework, the control analysis problem focuses on two key questions : first, is the system stable for all perturbations in some prescribed set (robust stability); and second, does the error remain in a desired bounded set for all perturbations and inputs in some appropriate sets (robust performance).

Practically speaking, this approach will be applied to plants with input signals of bounded energy or bounded power, and the results guarantee that the outputs are also bounded in energy or power, respectively. For the class of bounded energy signals, mild smoothness conditions guarantee that the signal goes to zero asymptotically. It should be noted that the class of input signals can be broadened by the inclusion of weights which are incorporated into the nominal plant M. This can be used, for example, to include steps in the input class. Similarly, the output signals can be weighted to incorporate performance criteria.

3.2 Stability and Performance Results

In this section, the results of [3] are briefly summarized. Consider again Figure 2 and an appropriate partitioning of M:

$$\begin{pmatrix} e \\ z \end{pmatrix} = \begin{pmatrix} M_{11} & M_{12} \\ M_{21} & M_{22} \end{pmatrix} \begin{pmatrix} v \\ w \end{pmatrix} \tag{13}$$

Connecting the loop between z and w yields the linear fractional transformation (LFT) representation for the overall operator G_Δ :

$$e = F_l(M, \Delta)v \triangleq [M_{11} + M_{12}\Delta(I - M_{22}\Delta)^{-1}M_{21}]v \tag{14}$$

Since it is required that the nonlinearities are conic sector bounded, it is without loss of generality that Δ is restricted to the class of bounded operators:

$$B\mathbf{\Delta} := \{\Delta \in \mathbf{\Delta} | \Delta \in \text{Cone}(0, \mathrm{I}, \mathrm{I})\} \tag{15}$$

We forgo formally defining a cone until the next section, it suffices to say that the operators in this class have well-behaved bounded properties. The small gain theorem can be used to arrive at sufficient conditions for robust stability and performance (RS) and (RP):

$$\begin{aligned} RS: &\quad \|M_{22}\|_\infty = \beta_{RS} \qquad (\beta_{RS} < 1) \\ RP: &\quad \|F_l(M, \Delta)\|_\infty = \beta_{RP} \quad (\beta_{RP} < 1) \text{ for all } \Delta \in B\mathbf{\Delta} \end{aligned} \tag{16}$$

These conservative conditions can be improved by the introduction of constant scaling matrices which commute with the perturbation block Δ. In this context, commutivity is defined to be:

$$\|D\Delta D^{-1}\|_\infty \leq \|\Delta\|_\infty \tag{17}$$

For the uncertainty structure given in equation (12), one appropriately structured commuting set is:

$$\begin{aligned} \mathcal{D} \triangleq &\{\text{diag}[D_1, \ldots, D_m, d_1 I_{k_1}, \ldots, d_n I_{k_n}] \\ &|D_i \in C^{r_i \times r_i} \text{ is invertible}, d_i \neq 0\} \end{aligned} \tag{18}$$

Incorporating these scaling matrices, we can arrive at less conservative conditions for Robust Stability and Robust Performance:

$$\begin{aligned} RS': &\quad \|DM_{22}D^{-1}\|_\infty = \beta_{RS'} \quad (\beta_{RS'} < 1) \\ RP': &\quad \|F_l\left(\left[\begin{pmatrix} I & 0 \\ 0 & D \end{pmatrix} M \begin{pmatrix} I & 0 \\ 0 & D^{-1} \end{pmatrix}\right], \Delta\right)\|_\infty = \beta_{RP'} \\ &(\beta_{RP'} < 1) \text{ for all } \Delta \in B\mathbf{\Delta} \end{aligned} \tag{19}$$

In [3], the motivation was presented for carrying out the SSV calculations in the time domain because of the computational attractiveness of the resulting calculations. Consider now the discrete map $N(z)$ which is calculated from $M(s)$ with the norm-preserving bilinear transformation $s = \frac{1-z}{1+z}$ mapping the unit disk to the right half plane. The map is appropriately partitioned :

$$\begin{pmatrix} x_{k+1} \\ e_k \\ z_k \end{pmatrix} = \begin{pmatrix} N_{11} & N_{12} & N_{13} \\ N_{21} & N_{22} & N_{23} \\ N_{31} & N_{32} & N_{33} \end{pmatrix} \begin{pmatrix} x_k \\ v_k \\ w_k \end{pmatrix} \tag{20}$$

where $w_k = \Delta(k, z_k)$ and for each k, Δ is an element of the prescribed uncertainty set $B\mathbf{\Delta}$. Now a coordinate transformation, $\hat{T}$, is introduced as a scaling on the state variables. In an analogous manner to the commuting D scales, the coordinate transformation reduces the conservatism of the time domain result.

Theorem 1 (Robust Performance) *Given a system N and block structure Δ. Suppose Δ is inside Cone(0,I,I). If there are appropriately partitioned constant scaling matrices $\hat{T}$ and D such that:*

$$\bar{\sigma}\left(\begin{pmatrix} \hat{T} & 0 & 0 \\ 0 & I & 0 \\ 0 & 0 & D \end{pmatrix} N \begin{pmatrix} \hat{T}^{-1} & 0 & 0 \\ 0 & I & 0 \\ 0 & 0 & D^{-1} \end{pmatrix}\right) = \beta < 1$$

then the uncertain system:

$$\begin{pmatrix} x_{k+1} \\ e_k \\ z_k \end{pmatrix} = \begin{pmatrix} N_{11} & N_{12} & N_{13} \\ N_{21} & N_{22} & N_{23} \\ N_{31} & N_{32} & N_{33} \end{pmatrix} \begin{pmatrix} x_k \\ v_k \\ w_k \end{pmatrix}$$

$$w_k = \Delta(k, z_k)$$

is zero-input exponentially stable and if $x_0 = 0$ and $\{v_k\}_{k=0}^\infty \in \ell_2$, then $\|e\|_{\ell_2} \leq \beta \|v\|_{\ell_2}$.

Proof *See [3].*

3.3 State Bounded Result

For this study, it is necessary to impose bounds on the state variables to guarantee the invertibility of the linearising transformations as well as to facilitate the calculation of conic sector bounds. The region will consist of a scaled unit hypersphere which becomes a hyperellipsoid in the original variables.

The SSV yields performance results with the norm of an error signal being bounded by a norm on the input signal. If we select as an error signal x_s, the scaled states, then we can calculate an upper bound for x_s as a function of the inputs and the initial conditions. This particular value of the SSV will be denoted β_{BS}:

$$\text{Theorem 1 and } \{v_k\}_{k=0}^\infty \in \ell_2 \Rightarrow \|x_s\|_{\ell_2}^2 \leq \beta_{BS}^2 \|v\|_{\ell_2}^2 + \|\tilde{x}_0\|_{\ell_2}^2$$

Here $\tilde{x}_0 = \hat{T}x_0$ represents the transformed states of the closed loop system. In order to consider only the original states of plant, a correction must be made for the transformation $\hat{T}$. If the initial controller states are chosen to be zero, then the tradeoff between the effect of initial conditions and input magnitude is given by the ellipse:

$$\|x_s\|_{\ell_2}^2 \leq \beta_{BS}^2 \|v\|_{\ell_2}^2 + \bar{\sigma}^2(\hat{T})\|x_{s0}\|_{\ell_2}^2 \leq 1 \tag{21}$$

The spatial result follows directly from this temporal norm bound and the fact that at a given k, $\|x_{sk}\|^2 \leq \sum_{k=1}^\infty \|x_{sk}\|^2 = \|x_s\|_{\ell_2}^2$.

4 Conic Sector Bounded Nonlinearities

4.1 General Description

In this section, the class of nonlinear operators which are to be considered is formally defined. It is required that the operator $y = N(x)$ be inside a conic sector or cone as defined by:

$$\text{Cone(C, R, S)} \triangleq \{(x,y) | y = Cx + S\Delta(Rx), \|\Delta(x)\| \leq \|x\|\} \quad (22)$$

For $y \in \Re^p, x \in \Re^n$ and a square Δ structure of size d, then $S \in \Re^{p \times d}, R \in \Re^{d \times n}$ and $C \in \Re^{p \times n}$. A simpler definition of a cone is given for the case where $S = I$:

$$\text{Cone(C, R, I)} \triangleq \{(x,y) | \|y - Cx\| \leq \|Rx\|\} \quad (23)$$

In simplest terms, the cone center C represents the best linear approximation of the nonlinear operator over the range of interest. The radii R and S give some measure of the error associated with this representation. A key point to note is that the Cone(C,R,S) contains many different operators, some of which may be considerably more pathological than the original nonlinear operator.

In terms of LFTs, the conic sector has a convenient representation which lends itself naturally to SSV analysis:

$$\text{Cone(C, R, S)} = F_u(M_c, \hat{\Delta}) \text{ where } M_c = \begin{pmatrix} 0 & R \\ S & C \end{pmatrix} \quad (24)$$

and $\hat{\Delta}$ is inside the Cone(0,I,I). This shows quite clearly how the nominal plant Cx is perturbed via the terms R and S. A minimization of these two factors yields the least "uncertain" or most linear system. The term R accounts for the interactions between the inputs to the operator and the term S takes into account the coupling between the outputs of the system. For example, a perfectly diagonal map such as $y_i = f_i(x)$ for $i = 1, p$ can be described by a cone with a diagonal R term and a diagonal Δ structure with p uncertain gains (the diagonal S term can be absorbed through the Δ block into the R term).

4.2 Optimal Cones

The objective of a minimally conservative paradigm is to reduce the effect of the $S\Delta R$ term in the conic sector description of our nonlinear plant. This is determined by two factors:

- The overall magnitude of R and S
- The complexity of the Δ structure

The balancing of these two factors to yield the least conservative SSV calculation is a formidable task, involving an elaborate iterative scheme. A simple algorithm is proposed here to arrive at a suboptimal solution to this problem (though not necessarily the global optimum).

In general, the maximum (sensible) Δ is a diagonal matrix containing np independent gains. This assumes completely independent gains for each input-output matching in the mapping of N. At the other extreme, the simplest nonlinear operator could be described with a single uncertain gain. This is true in the conic sector representation for the dynamics of a simple CSTR [3]. Simpler Δ structures are more attractive from a computational perspective, and in fact the SSV is equal to its computable upper bound for some simple structures in the case where Δ is linear (but possibly time-varying) [11].

For a fixed Δ structure, a simple geometric argument will be made for the definition of a minimally conservative cone. Consider the case of a scalar nonlinear operator ($S = 1$). In the table below is shown the geometric interpretation of various conic sectors. In order to minimize the region inside the cone, one can minimize the hyperdimensional angle (or sum of such quantities) which define the region. It can be shown that this is equivalent to a minimization of the Frobenius norm of the matrix R. This result can also be derived from the fact that the Frobenius norm is an upper bound for the infinity norm. Using the conic sector definition (22) we get:

$$\frac{\|S\Delta(Rx)\|}{\|x\|^2} \leq \frac{\|S\|\|\Delta(Rx)\|}{\|x\|^2} \leq \frac{\|S\|\|Rx\|}{\|x\|^2} \leq \|S\|_F \|R\|_F \quad (25)$$

Conic Sector Regions		
d	n	Region
1	1	2 Flat Slices
1	2	2 Infinitely Deep Slices
2	2	2 Square Based Pyramids

Table 1

Three possibly distinct solutions to the conic sector minimization problem can be envisioned corresponding to three Δ structures. The *Feasible* solution minimizes the Frobenius norm of the smallest Δ structure which can envelop the nonlinear operator. The *Full* solution minimizes the Frobenius norm of the largest sensible Δ structure (np independent gains). As the size of the Δ structure increases, the Frobenius norm must necessarily decrease (i.e. the smaller Feasible structures are all subsets of a larger structure). As these are the limiting cases, the *Global Optimal* solution, which minimizes the upper bound on the SSV must lie between them. The tradeoff between simple Δ structure and small Frobenius norm is balanced at this point.

4.3 Numerical Calculations

A nonlinear program (NLP) is set up to calculate the solution which minimizes the Frobenius norm for a given Δ structure. The program requires q data points consisting of an input vector x and corresponding output vector y. As most of the nonlinearities for this study are monotonic and constrained to a finite region in x, it was often sufficient to calculate the data points along the boundary of the hyper-ellipsoid. The general scheme of the the NLP is to minimize the Frobenius norm with the constraint that the data lie inside the calculated conic sector. Obviously, the larger the value of q, the more accurate the calculated conic sector and the greater the computational complexity of the NLP. For the case where the d sub-blocks of Δ are scalar, the NLP can be written:

$$\text{Min } \eta$$

$$\left(\sqrt{\sum_{i=1}^{p}\sum_{j=1}^{d} S_{ij}^2}\right)\left(\sqrt{\sum_{i=1}^{d}\sum_{j=1}^{n} R_{ij}^2}\right) = \eta$$

$$k = 1, q \begin{cases} \sum_{i=1}^{n} C_{1i}x_{ik} + \sum_{i=1}^{d}\left[S_{1i}\left(\sum_{j=1}^{n} R_{ij}x_{jk}\right)\delta_{ik}\right] & = y_{1k} \\ \vdots & \\ \sum_{i=1}^{n} C_{pi}x_{ik} + \sum_{i=1}^{d}\left[S_{pi}\left(\sum_{j=1}^{n} R_{ij}x_{jk}\right)\delta_{ik}\right] & = y_{pk} \\ |\delta_{1k}| & \leq 1 \\ \vdots & \\ |\delta_{dk}| & \leq 1 \end{cases}$$

where $\{(y_{1i}, \ldots, y_{pi}), (x_{1i}, \ldots, x_{ni})\}$ are the given data points ($i = 1, q$). The total number of variables is $(1 + dn + dp + pn + dq)$ and the total number of constraints is $(1 + pq + dq)$. It is important to note that the above algorithm can be used to find the linear bounds on an arbitrary polynomial approximation (cone center) to the nonlinear function. The additional variables introduced appear linearly in the constraint equations (i.e. $y = C_1x + C_2x^2 + \cdots$). This approach will be used in conjunction with the QAL scheme.

5 Application to a Nonlinear CSTR

5.1 CSTR Model

The mass and energy balances for a CSTR with first order, irreversible, exothermic kinetics ($A \rightarrow B$) are give by :

$$\begin{aligned} \dot{\tilde{x}}_1 &= \tilde{f}_1 = -\tilde{x}_1 - x_{10} + \mathcal{D}a(1 - \tilde{x}_1 - x_{10})e^{\frac{\tilde{x}_2 + x_{20}}{1 + (\tilde{x}_2 + x_{20})/\gamma}} \\ \dot{\tilde{x}}_2 &= \tilde{f}_2 - \beta u + d = -\tilde{x}_2 - x_{20} - \beta(\tilde{u} + u_0) + d \\ &\quad + B\mathcal{D}a(1 - \tilde{x}_1 - x_{10})e^{\frac{\tilde{x}_2 + x_{20}}{1 + (\tilde{x}_2 + x_{20})/\gamma}} - \beta(\tilde{x}_2 + x_{20}) \end{aligned} \quad (26)$$

(using the dimensionless quantities defined in the nomenclature). This simple model has two state variables (reactant concentration, reactor temperature). The control problem focuses on the SISO regulation of the reactor temperature by manipulating the cooling water temperature while subjected to disturbances in the feed stream temperature. The values of the dimensionless parameters

are [1]: $\mathcal{D}a = 0.072, B = 8, \beta = 0.3, \gamma = 20$ and $x_c = 0.0$. These conditions lead to multiple steady states and operation is chosen at the unstable point : $(u_0 = -0.20, x_{10} = 0.5, x_{20} = 3.03)$.

5.2 Linearizing Transformations and Uncertainty Description

We consider three controller synthesis techniques (GSL, QAL and simple linear (P, PI)) as well as 2 disturbance classes (bounded energy and steps). The results are extensively documented in [2]. The GSL results have been published elsewhere [1],[4], we merely summarize here. The state and input transformations :

$$\begin{aligned} z_1 = \quad & T_1(x) = \quad x_1 - x_{10} \\ z_2 = \quad & T_2(x) = \quad \tilde{f}_1(x_1 - x_{10}) \\ \alpha(x) = \quad & < dT_2, f > \\ \beta(x) = \quad & < dT_2, g > -I \end{aligned} \tag{27}$$

yield, in transformed coordinates, the dynamical system:

$$\dot{z} = \begin{pmatrix} 0 & 1 \\ 0 & 0 \end{pmatrix} z + \begin{pmatrix} 0 \\ 1 \end{pmatrix} v + \begin{pmatrix} \dfrac{0}{\dfrac{(x_2+x_1+x_{10})d}{\left[1+\dfrac{1}{\frac{x_2+x_1+x_{10}}{2\alpha(1-x_1-x_{10})}-1}\right]^2}} \end{pmatrix} \tag{28}$$

It is clear to see the constraints imposed by inverting $T_2(x)$ in equation (27). For general problems, this inherent limitation restricts the application of state linearization techniques to local regions in the phase space. For the purpose of this study, we consider the region of interest to be the interior of the ellipse:

$$\frac{z_1^2}{.08^2} + \frac{z_2^2}{.55^2} = 1 \tag{29}$$

for QAL. This corresponds roughly to a circle of radius 0.1 in the z domain for GSL.

For the QAL, it is necessary to calculate a nominal quadratic plant. Using the NLP described in the previous section, it is found that the *second* order plant with the tightest conic sector over the region of interest (equation (29)) is given by:

$$\begin{aligned} \dot{\tilde{x}}_1 &= -2\tilde{x}_1 + .381\tilde{x}_2 + .020\tilde{x}_1^2 - .761\tilde{x}_1\tilde{x}_2 + .127\tilde{x}_2^2 \\ \dot{\tilde{x}}_2 &= -8\tilde{x}_1 + 1.75\tilde{x}_2 + .320\tilde{x}_1^2 - 6.09\tilde{x}_1\tilde{x}_2 + 1.02\tilde{x}_2^2 + 0.3\tilde{u} \end{aligned} \tag{30}$$

The uncertainty is characterized by a single uncertain gain with radii: $S = (1 \quad 8)^T, R = (0 \quad 0.0067)$. This can be compared with the tightest conic sector associated with a *first* order approximation of the nonlinear plant:

$$\dot{\tilde{x}} = \begin{pmatrix} -2 & 0.377 \\ -8 & 1.718 \end{pmatrix} \tilde{x} + \begin{pmatrix} 1 \\ 0.3 \end{pmatrix} \tilde{u} \tag{31}$$

and its associated uncertainty radii: $S = (1 \quad 8)^T, R = (0 \quad 0.104)$. Using the objective in our NLP as a measure, the quadratic approximation reduces the nonlinear uncertainty by a factor of 15. The second order system in equation (30) yields an exact quadratic linearization with the following state and input transformations :

$$\begin{aligned} z_1 = T_1(x) = \quad & \tilde{x}_1 \quad -0.7388\tilde{x}_1^2 \\ z_2 = T_2(x) = \quad & \tilde{x}_2 \quad +3.9320\tilde{x}_1^2 - 3.4751\tilde{x}_1\tilde{x}_2 + 0.3333\tilde{x}_2^2 \\ \alpha(x) = \quad & \quad -1.3304\tilde{x}_1^2 - 4.9235\tilde{x}_1\tilde{x}_2 + 0.9311\tilde{x}_2^2 \\ \beta(x) = \quad & \quad -3.4751\tilde{x}_1 + 0.6667\tilde{x}_2 \end{aligned} \tag{32}$$

In the transformed coordinates we have the same linear approximation:

$$\dot{z} = \begin{pmatrix} -2 & 0.3808 \\ -8 & 1.7467 \end{pmatrix} z + \begin{pmatrix} 0 \\ 0.3 \end{pmatrix} v + \left[\frac{\partial T}{\partial x}\begin{pmatrix} 0 \\ d \end{pmatrix}\right]_{x=T^{-1}(z)} + \Delta P \tag{33}$$

where the Jacobian is calculated from equation (32). The quadratic transformation is also invertible over the region defined in equation (29). The other term in this equation, ΔP, accounts for both the error in approximating the nonlinear plant by a second order system and also for the order 3 and higher terms inherent in the QAL.

In summary for the disturbance problem, the GSL scheme requires a single uncertainty block to represent the nonlinear effect of the disturbance. This block is optimally modeled with two uncertain nonlinear gains. The QAL technique requires an uncertainty block for both the nonlinear disturbance effect and the plant modeling error. In this case, the optimal uncertainty description has three nonlinear gains. Finally, the simple linear control approach requires a single uncertain gain to represent the error inherent in the first order approximation. The structure of the various uncertainty blocks and the magnitude of their radii are listed in the table below. It should be pointed out that conclusions about the various schemes based on these data alone should be drawn carefully. The schemes represent rather different coordinate systems as well as uncertainty structures.

Uncertainty Descriptions		
Method	Δ structure	$\|S\|_F\|R\|_F$
GSL	$\begin{pmatrix} \delta_1 & 0 \\ 0 & \delta_2 \end{pmatrix}$	0.29
QAL	$\begin{pmatrix} \delta_1 & 0 & 0 \\ 0 & \delta_2 & 0 \\ 0 & 0 & \delta_3 \end{pmatrix}$	0.61
Linear	(δ_1)	1.10

Table 2

5.3 Analysis of Stability Properties

We restrict our attention in this paper to a particular performance criterion - namely the bounding of the states while the plant is subjected to two classes of disturbances. In the first case, we consider bounded inputs of bounded energy (e.g. decaying sinusoids). In the second case, we consider the class of inputs of bounded energy passed through the filter $\frac{1}{s}$ (e.g. steps).

5.3.1 Bounded Energy Disturbances

In this case it is sufficient to consider simple proportional control in the outer loop of Figure 1. No integral action is required for feed temperature disturbances of bounded energy to guarantee zero offset. The controller gains [1.35, 2.12] as found in [1] are used for the GSL, and the gains [−16.9, 6.23] yield the same closed loop poles for the QAL (and the simple linear approach). To simplify our comparison, we allow all three systems to have the same closed loop dynamics in the *transformed* variables. A more realistic comparison might involve calculating a controller to give the same dynamics in the original variables but as we have seen (sec. 2.1) this is not easily done for the GSL.

The analysis procedure involves varying the magnitude of d and calculating a corresponding value of β_{BS}. Then we can use equation (21) to calculate a bound on the initial state. For the general robust performance problem, one can use this approach to calculate the tradeoff between initial condition and input magnitude effects on the computed performance guarantee. For the state bound problem, the tradeoff curves are plotted in Figure 3. Recall that this approach yields sufficient results, so the curves in this diagram represent a lower bound on the tolerable disturbance and initial condition magnitudes which give rise to bounded states. An additional point is given in the diagram to show an actual simulation in which the states escape the bound in (29). This represents an upper bound on the tolerable disturbance magnitude (zero initial condition) and the proximity of the points along the y-axis shows the promise of this technique.

In Figure 4, we depict the various state bounds as they are mapped into the true $x_1 - x_2$ coordinate system. As expected, the QAL contour shows minimal deformation of the original ellipse as compared to the GSL contour. It is evident from this figure that a precise comparison of the results is not possible. Each result guarantees stability over a different region in the phase space. Included in this diagram is the phase portrait of the response of the simple linear system to the input disturbance $0.3\,e^{-.25t}\sin(.5t)$. The response of the QAL and GSL are virtually identical to the depicted response for this input. This indicates that Table 2 is a reasonable measure of the conservatism inherent in analyzing the three approaches in the SSV framework.

5.3.2 Step Inputs

The above procedure is repeated for persistent step disturbances with PI control in the outer loop for aysymptotic tracking. The

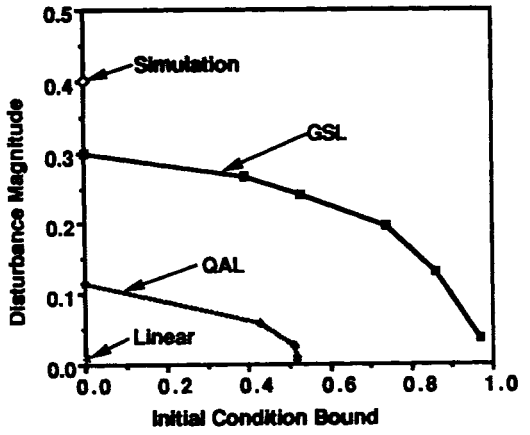

Figure 3: Bounds for which closed loop stability is guaranteed (Bounded $\mathcal{L}_2$ Signals)

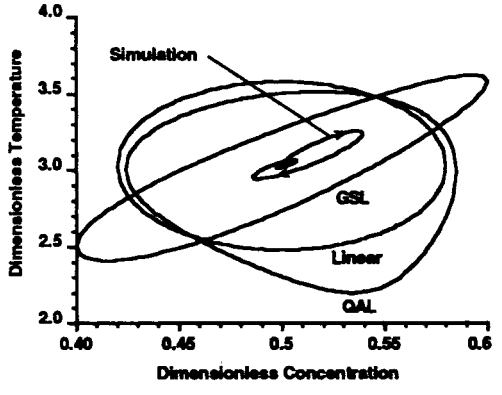

Figure 4: Bounds on State Trajectories

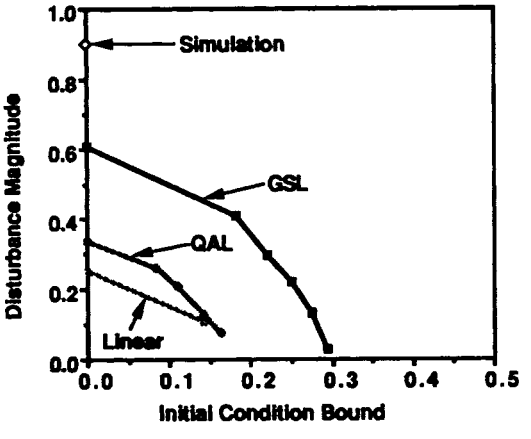

Figure 5: Bounds for which closed loop stability is guaranteed (Step-like Signals)

controller gains are $[4.93, 3.93]$ for the GSL and the error in z_1 is integrated with $\tau_I = 0.422$. For the QAL (and linear) schemes, the gains which yield the same closed loop poles are $[-17.27, 12.25]$ and $\tau_I = 0.0482$. The GSL approach suffers from the weakness that only z_1 represents a physically meaningful quantity to integrate. This is opposed to the flexibility inherent in the QAL scheme to integrate a reasonable estimate of x_2. The tradeoff between disturbance bounds and initial condition magnitudes is shown in Figure 5.

6 Conclusion

In this paper we have revealed the theoretical concepts which demonstrate that the Quadratic Approximate Linearization is a more practical linearization scheme than the Global State Linearization. The presence of external disturbances and unmodeled dynamics is manifested in relatively minimal nonlinear behavior in the QAL scheme. In addition, the broad applicability of this technique and potential for systematic optimization of the resultant solution further motivate its use. Coupled with extensions of the SSV to nonlinear systems, a control design procedure is developed which enables the analysis of stability and performance properties for these linearization schemes.

Acknowledgements

The authors wish to thank Sinan Karahan for providing us with a preliminary version of the MATLAB software for Approximate Linearization.

References

[1] Calvet, J.P., "A Differential Geometric Approach for the Nominal and Robust Control of Nonlinear Chemical Processes", Ph.D. Thesis, Georgia Institute of Technology, Atlanta, GA, 1989.

[2] Doyle III, F. J. and Morari, M., "Nonlinear Controller Design and Analysis for Uncertain Process Systems", in preparation, 1990.

[3] Doyle III, F. J., A. P. Packard and M. Morari, "Robust Controller Design for a Nonlinear CSTR", Chem. Eng. Sci., **44**, 1929-1947, 1989.

[4] Hoo, K. A. and Kantor, J.C., "An Exothermic Continuous Stirred Tank Reactor is Feedback Equivalent to a Linear System", Chem. Eng. Comm., **37**, 1-10, 1985.

[5] Hunt, L.R., Su, R., and Meyer, G.,"Global Transformations of Nonlinear Systems", IEEE Trans. Aut. Control, **24**, 24-31, 1983.

[6] Isidori, A., *Nonlinear Control Systems*, Springer-Verlag, New York, NY, 1989.

[7] Karahan, S., "Higher Degree Approximations to Nonlinear Systems", Ph.D., University of California, Davis, CA, 1988.

[8] Kravaris, C. and Kantor, J.C., "Geometric Methods for Nonlinear Process Control: A Tutorial", I. & E.C. Res., in press, 1990.

[9] Krener, A.J., "Approximate Linearization by State Feedback and Coordinate Change", Syst. Contr. Lett, **5**, 181-185, 1984.

[10] Packard, A., "What's New with μ: Structured Uncertainty in Multivariable Control", Ph.D. Thesis, University of California, Berkeley, CA, 1987.

[11] Packard, A. and Doyle, J., "Structured Singular Value with Repeated Scalar Blocks", Proc. 1988 Am. Contr. Conf., 1213-1218.

7 Nomenclature

B	$-\Delta H C_{Af}/C_p T_{f_0} \gamma$	T_{c_0}	nominal coolant temp
C_A	reactant conc.	T_f	actual feed temp
C_p	heat capacity	T_{f_0}	nominal feed temp
$\mathcal{D}a$	$\frac{V}{Q_f} k_0 e^{-\gamma}$	U	heat transfer coeff.
$\mathcal{D}a_1$	$\frac{V}{Q_f} k_1$	V	reactor volume
$\mathcal{D}a_2$	$\frac{V}{Q_f} k_2 C_{Af}$	u	$(T_c - T_{c_0})/T_{f_0}\gamma$
$\mathcal{D}a_3$	$\frac{V}{Q_f} k_3 C_{Af}$	u_f	recycle fraction
$\mathcal{D}a_4$	$\frac{V}{Q_f} k_4$	x_a	$\frac{C_A}{C_{Af}}$
d	$(T_f - T_{f_0})/T_{f_0}\gamma$	x_b	$\frac{C_B}{C_{Af}}$
Ea	activation energy	x_c	$\frac{C_C}{C_{Af}}$
ΔH	heat of reaction	x_1	$(C_{Af} - C_A)/C_A$
k_0	rate constant	x_2	$(T - T_{f_0})/T_{f_0}\gamma$
Q_f	feed stream flow rate	β	$UA_h/Q_f C_p$
R	ideal gas constant	γ	Ea/RT_{f_0}
T_c	coolant temp	λ_i	purity of i